COBEM 2023 27TH INTERNATIONAL CONGRESS OF MECHANICAL ENGINEERING

ABCM Brazilian Society of Mechanical Sciences and Engineering
27th ABCM International Congress of Mechanical Engineering
December 04-08, 2023, Florianópolis-SC, Brazil

# COB-2023-0456
# DETERMINATION OF THE REINFORCEMENT STEEL AREA IN PURE BENDING CONSIDERING THE STRESS-STRAIN DIAGRAM WITH THE CREEP OF CONCRETE

**Rodrigo Oliveira da Silva Conceição**
Institutional Scientific Initiation Program (PIBIC), Department of Construction and Structures, Polytechnic School, Federal University of Bahia (UFBA), Aristides Novis Street, 02, 5th floor – Federação, Salvador – 40.210-910, Bahia, Brazil
rodrigoosc@ufba.br

**Alexandre de Macêdo Wahrhaftig**
Department of Construction and Structures, Polytechnic School, Federal University of Bahia (UFBA), Aristides Novis Street, 02, 5th floor – Federação, Salvador – 40.210-910, Bahia, Brazil
alixa@ufba.br

**Iago Gonçalves de Oliveira**
Institutional Scientific Initiation Program (PIBIC), Department of Construction and Structures, Polytechnic School, Federal University of Bahia (UFBA), Aristides Novis Street, 02, 5th floor – Federação, Salvador – 40.210-910, Bahia, Brazil
iagogo@ufba.br

**Cibele Mota Menezes**
Graduate Program in Civil Engineering (PPEC), Polytechnic School, Federal University of Bahia (UFBA), Aristides Novis Street, 02, 8th floor, Federação, Salvador – 40.210-910, Bahia, Brazil
cibele.menezes@ufba.br

***Abstract.*** *When dimensioning the reinforced concrete structures, the engineer establishes an area of reinforcement steel intending to, together with the compressed region of concrete, find the balance of the analyzed section. Concrete is a brittle material and therefore does not have high tensile strength. For this reason, the introduction of reinforcement bars in tensioned region is necessary so that the balance of the section is established. In this context, the knowledge of the stress-strain diagram of materials is essential. In the case of concrete, its viscoelastic behavior still needs to be observed in that context. Viscoelastic materials exhibit creep, characterized by the increase of strains over time, even if the stress level is maintained unchanged. Creep modifies the stress-strain diagram of the concrete and, therefore, the internal lever arm that defines the balance of forces in the section. In this work, the calculation of the reinforcement steel area of sections in pure bending is studied by taking the stress-strain diagram of the concrete modified by the creep of the material. A rectangular section, submitted exclusively to the action of a positive bending moment, is examined. The definition of the reinforcement steel area is done for different time instants.*

***Keywords:*** *Reinforced concrete structures, Stress-strain diagram, Pure bending, Creep of concrete, Reinforcement steel area.*

## 1. INTRODUCTION

Reinforced concrete is a composite material widely used in civil construction sectors, which combines concrete with, in most cases, steel bars. The union of these two materials, with different mechanical characteristics, creates conditions for structures in bending to be durable, resistant, and able to overcome large spans with relative economy and efficiency. This is due to the combination of the mechanical properties of each of these materials. While concrete resists well to compression, steel resists to both tensile and compressive stresses. Song and Hwang (2004) state that the brittle aspect of concrete, which results in low tensile strength and low deformation capacity, can be compensated by adding steel reinforcement.

In the dimensioning of reinforced concrete structures, the project engineer starts his work by conceiving a structural arrangement, then accounts for the loads and subsequently performs the calculations considering preliminary dimensions of a cross section. The aim is to establish a steel area that can lead, together with the compressed region of the concrete, to the balance of the analyzed section.

Concrete is a brittle breaking material and therefore does not have a high tensile strength. Even its small resistance is usually disregarded for design purposes. During the bending, a positive bending moment, for example, causes tension in the fibers below the neutral line and compression in the superior ones. For this reason, the introduction of steel bars in the tensioned region is necessary for the cross section to be balanced. This balance occurs due to the formation of internal forces that are mobilized due to the presence of steel and concrete. Horizontally, these forces compensate each other because they are coplanar, but their positions are not collinear. This means that there is a distance, or lever arm, between the resultant of tension, in the reinforcement, and that of compression, in the concrete. This gives rise to an internal moment capable of promoting the cross-section equilibrium with respect to rotation. As the tensile strength is calculated by the product between the yield stress of the steel and the total area of the reinforcement, the required area of steel is calculated.

In this process, the knowledge of the stress-strain curve of the materials is essential. In the case of concrete, its viscoelastic behavior still needs to be observed. Viscoelastic materials exhibit creep, characterized by the increase in deformations over time, even if the level of stress is kept unchanged. This phenomenon occurs predominantly due to the movement of water in the voids present inside the hardened concrete mass. Creep modifies the concrete stress-strain curve and, therefore, the lever arm that defines the cross-section equilibrium. For this reason, the definition of the steel reinforcement area of structures in bending should be made based on the concrete stress-strain diagram modified by the creep of the material, as well as other properties that are intrinsic to it (Nicoletti et al., 2022). In this sense, in the design of reinforced concrete parts, it is essential to have technical considerations and calculation routines that guide the verification and design processes within the scope of structural analysis. The definition of the type of steel and concrete, and the determination of loads are fundamental in this process. According to Giorlaa and Dunantb (2018), it is necessary to know the short-and long-term behavior of concrete, including its viscous properties, since these change the initial design conditions.

Creep is a physical phenomenon characterized by progressive deformation as a function of time, even under constant loading (ACI-209R-08, 2008). This phenomenon occurs due to gradual atomic rearrangements inside the materials and the movement of retained water after the hardening of the fluid mass. The atomic rearrangement, the shape of the aggregates, and the movement of water between voids can potentiate this phenomenon. Su et al. (2017) call the attention for the fact that the creep behavior of concrete has not yet been fully studied. Pena et al. (2022) state that creep deformations are the reflection of internal micro-mechanisms that occur in concrete structural elements when they are loaded. According to Zhou et al. (2022), the creep deformation of concrete is subject, among other aspects, to the duration in which the load is applied. On the other hand, Wei et al. (2018) state that creep also depends on the type of loading that the parts of concrete are subjected to. Creep reduces the product of inertia of structural concrete components in bending when subjected to long-term loading (Elaghoury and Bartlett, 2019).

In general, concrete structures are exposed to environmental conditions, and therefore subject to variation in humidity and temperature levels. These factors directly interfere with the occurrence of creep (Magalhães et al., 2022). Other aspects such as the high water/aggregate ratio and low concrete strength are also determining factors. According to Yu et al. (2020), when concrete is subjected to elevated temperatures, there is an increase in the rupture speed of the material microstructures, which enhances the phenomenon. Zamaliev and Zakirov (2018) confirmed this mechanism when analyzing the stress-strain state formed in reinforced concrete slabs when subjected to long-term loading. In turn, Boumakis et al. (2018) affirm that that the creep of concrete is a phenomenon that directly contributes to the decrease in durability of structures made with this material.

In the context of what was previously exposed, the present article aims to evaluate the steel reinforcement area required for a reinforced concrete beam in pure bending, taking into account the concrete creep in the balance of internal forces in the section. For this, a rectangular section, submitted exclusively to the action of a positive bending moment, is examined in the definition of the steel area considering different instants of time.

## 2. CONCRETE STRESS-STRAIN DIAGRAM CONSIDERING CREEP

When dimensioning reinforced concrete cross sections, the primary objective is to find the area of reinforcement steel required for the part to resist the forces to which it is subjected. Steel and concrete work together to produce the balance of the cross sections. In general, concrete is responsible for holding compressive stresses and steel the tensile stresses. To size the steel area, it is necessary to know the stress-strain diagrams of the two materials, and their inverse, in the case of concrete.

In case of concrete, it is also necessary to consider the creep of the material, since it produces changes in the original diagram that is defined for the initial instant of loading. This makes the analysis become time-dependent, since the strain-stress diagram of concrete becomes a time function due to the gradual increase in strains. Time-dependent movements in structural concrete indicate that there is a continuous change in strains regimen, with stress transfer from one material to another (Ali and Forth, 2023). Figure 1 presents the stress-strain and strain-stress diagrams of concrete, letters (a) and (b), respectively, by considering the creep phenomenon, there represented by the so-called creep coefficient, $\phi(t)$.

The curve that represents the stress-strain diagram of concrete can be divided into three well-defined parts, which are related to the distinct stages of the mechanical behavior of the material. First, there is a stretch linear corresponding to the elastic behavior, followed by a typically nonlinear one and continued by a third phase, which characterizes the plastic behavior of the material, which extends to the ultimate limit state.

The elastic state, therefore, is composed of two phases: the linear elastic and the non-linear elastic phase. In the linear elastic phase, the stress increases proportionally to strain up to $\varepsilon_{c1}$, and Hooke's Law can be observed (Magalhães et al., 2022). In the non-linear elastic phase, the relationships between stresses and strains are no longer proportional, and the curve assumes a parabolic shape up to $\varepsilon_{c2}$. At this stage, the first micro-cracks appear inside the material.

In the plastic state, the concrete strength reaches its maximum value at $\varepsilon_{c2}$. Beyond this value, pre-existing and new micro-cracks increase in size and accumulate, becoming larger cracks due to the increase of stresses at the ends of the micro-cracks. In this state, the concrete loses a large part of its resistive capacity and is no longer able to recover its original state. At this point, the structure begins to show visible signs of failure. The end of the plastic state is known as the ultimate limit state and occurs at $\varepsilon_{cu}$. In the ultimate limit state, there is a general failure of the concrete, which occurs in a fragile way, without prior notice, due to the progressive growth of cracks.

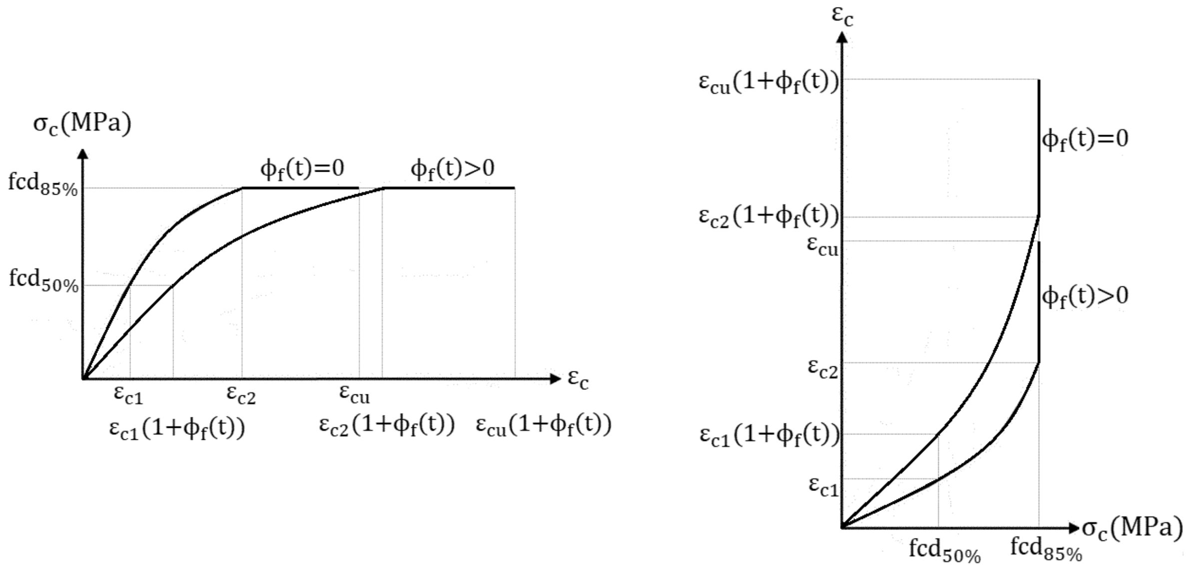


(a) (b)

Figure 1. Stress-strain (a) and strain-stress (b) diagrams illustration creep considering.

According to ABNT NBR 6118:2014, the linear elastic phase is valid up to 50% of the design strength of concrete, $f_{cd}$. The non-linear elastic phase is comprised between 50% and 85% of the design strength of concrete, that is, $0.5f_{cd}$ and $0.85f_{cd}$. The plastic state is comprised between the strain at the initial point of yielding, $\varepsilon_{c2}$, and the ultimate concrete strain, $\varepsilon_{cu}$. Finally, the ultimate limit state occurs at the point of rupture, i.e., at the ultimate strain of concrete.

## 3. MATHEMATICAL PROCEDURE

To obtain the reinforcement steel area, it is necessary to use the equation that defines the stress-strain diagram of concrete provided by ABNT NBR 6118:2014, described by Eq. (1):

$$\sigma_c = \begin{cases} 0.85 f_{cd}\left[1-\left(1-\dfrac{\varepsilon_c}{\varepsilon_{c2}}\right)^n\right], & 0 < \varepsilon_c \leq \varepsilon_{c2} \\ 0.85 f_{cd}, & \varepsilon_{c2} < \varepsilon_c \leq \varepsilon_{cu} \end{cases} \quad (1)$$

whose inverse relationship is given by Eq. (2):

$$\varepsilon_c = \begin{cases} \varepsilon_{c2}[1-\left(\sqrt[n]{1-\dfrac{\sigma_c}{0.85 f_{cd}}}\right)], & 0 < \sigma_c < 0.85 f_{cd} \\ \varepsilon_{c2} \leq \varepsilon_c \leq \varepsilon_{cu}, & \sigma_c = 0.85 f_{cd} \end{cases} \quad (2)$$

where:

$$f_{cd} = \frac{f_{ck}}{\gamma_c} \quad (3)$$

$f_{cd}$ is the design strength of concrete, which is equivalent to its characteristic strength, $f_{ck}$, reduced by a safety factor, $\gamma_c$, which considers the uncertainties regarding the material. In the previous equations, $\sigma_c$ and $\varepsilon_c$ are, respectively, the concrete stress and strain, with $n = 2$ admitted for concrete with characteristic strengths up to 50 MPa. According to ABNT NBR 6118, $\varepsilon_{c2} = 2‰$, $\varepsilon_{cu} = 3.5‰$ and $\gamma_c = 1.4$.

After defining the diagram, it is necessary to calculate the area below the curve, $A_d$, and the position of the centroid, $\overline{\varepsilon_c}$, to establish, respectively, the contribution of the compressed portion of the concrete and the distance of this portion to the neutral line, which is done in the form of Eqs (4) and (5), respectively:

$$A_d = \int_0^{\varepsilon_{cu}} \varepsilon_c d\varepsilon_c \tag{4}$$

$$\overline{\varepsilon_c} = \frac{\int_0^{\varepsilon_{cu}} \varepsilon_c \sigma_c d\varepsilon_c}{\int_0^{\varepsilon_{cu}} \varepsilon_c d\varepsilon_c} \tag{5}$$

After carrying out the corresponding integrations, Eqs (6) and (7) are found for the area and the centroid of the diagram, respectively:

$$A_d = 0.85 f_{cd}(\varepsilon_{cu} - \varepsilon_{c2}) + 0.85 f_{cd}[\varepsilon_{c2}(1 - \frac{1}{n+1})] \tag{6}$$

$$\overline{\varepsilon_c} = \frac{\varepsilon_{cu}{}^2 n^2 + 2\varepsilon_{cu}{}^2 - 2\varepsilon_{c2}{}^2 + 3n\varepsilon_{cu}{}^2}{2(n+2)(\varepsilon_{cu} - \varepsilon_{c2} + n\varepsilon_{cu})} \tag{7}$$

As seen, Eq. (6) defines the area below the curve of the strain-stress diagram of Figure 1(b), which represents the distribution of stresses in the compressed region of the section. On the other hand, Eq. (7) defines the centroid of this same curve, that is the place where the resultant of these stresses is sheltered, and consequently, its lever arm in relation to the geometric center of the reinforcement to be positioned in the tensioned region. With the introduction of concrete creep, the physical parameter portrayed in the equations, affected by this phenomenon, is the concrete strain, $\varepsilon_c$, which becomes a time-dependent quantity. This promotes changes in both, the area of the diagram and in the position of its centroid. According to Magalhães et al. (2023), when implementing creep strains in concrete, there will be an important change in the constitutive relationship of the material, because creep modifies the stress-strain relationship of the concrete.

In order to determine the creep strains, it is important to take into account the slow and fast strain of concrete. The rapid strain is irreversible and occurs during the first twenty-four hours after the structure is subjected to loading. On the other hand, slow strain can be irreversible or reversible. The total strain of concrete, $\varepsilon_c(t)$, which includes the creep portion, is calculated by:

$$\varepsilon_c(t) = \varepsilon_c(1 + \emptyset_f(t)) \tag{8}$$

where the creep coefficient, $\phi(t)$ is composed of three parts in order to include, respectively, the fast, slow irreversible and slow reversible deformations associated with the phenomenon. Thus, it is possible to write that:

$$\emptyset_f(t) = \emptyset_a(t) + \emptyset_b(t) + \emptyset_c(t) \tag{9}$$

The creep coefficient parcels are defined in the set of equations from (10) to (16).

$$\emptyset_a(t) = 0.8[\frac{e^{0,38(1-\sqrt{\frac{28}{t}})} - 1}{e^{0,38(1-\sqrt{\frac{28}{t}})}}] \tag{10}$$

$$\emptyset_b(t) = (4.45 - 0.035H)\left(\frac{A_{cs}e^{-7.8+0.1H} + 42P_{cs} + 21}{A_{cs}e^{-7.8+0.1H} + 20P_{cs} + 21}\right)[(\frac{t^2 + 40t + A}{t^2 + Bt + C}) - (\frac{A + 1904}{28B + C + 784})] \tag{11}$$

$$A = 116th_{fic}{}^3 - 282th_{fic}{}^2 + 220th_{fic} - 4.8 \tag{12}$$

$$B = 2.5th_{fic}^{\ 3} - 8.8th_{fic} + 40.7 \tag{13}$$

$$C = -75th_{fic}^{\ 3} + 582th_{fic}^{\ 2} + 496th_{fic} - 6.8 \tag{14}$$

$$th_{fic} = \frac{21 + A_{cs}e^{-7.8+0.1H}}{P_{cs}} \tag{15}$$

$$\emptyset_c(t) = 0.4[\frac{t-8}{t+42}] \tag{16}$$

where $t$ is the time when the analysis is performed; $t_0$ is the initial time, or the loading time, which, in the present case, is adopted as being 28 days after the production of the material; $H$ represents the ambient humidity, in percentage; $A_{cs}$ is the area of the concrete section; $P_{cs}$ is the perimeter of the section in contact with the environment; and $th_{fic}$ is the fictitious thickness.

After defining the creep coefficients, it is possible to obtain the total strain of the concrete and, consequently, to promote changes in the strain-strain curves, and vice-versa, and calculate the new areas and their centroids at the instant when the analysis should be performed. For this, it is necessary to rewrite Eq. (2) in terms of Eq. (8):

$$\varepsilon_c(t) = \begin{cases} \varepsilon_{c2}(1+\emptyset_f(t))[1-\left(\sqrt[n]{1-\dfrac{\sigma_c}{0.85f_{cd}}}\right)], & 0 < \sigma_c < 0.85f_{cd} \\ \varepsilon_{c2}(1+\emptyset_f(t)) \le \varepsilon_c \le \varepsilon_{cu}(1+\emptyset_f(t)), & \sigma_c = 0.85f_{cd} \end{cases} \tag{17}$$

With this, it is possible to obtain the area below the curve and the centroid for different time instants throughout the aging of the structure. On the other hand, for dimensioning the reinforcement steel area, as recommended, it is necessary to define the design strength of the steel, $f_{sd}$, used in the reinforcement, which is done in accordance with Eq. (18):

$$f_{sd} = \frac{f_{sk}}{\gamma_s} \tag{18}$$

where $\gamma s$ is the material safety factor, defined as 1.15.

The design bending moment, $M_d$, is established by increasing the characteristic value of the force, $M$, by a safety factor, $\gamma_m$, related to permanent actions, which is 1.4, according to Eq. (19):

$$M_d = \gamma_m M \tag{19}$$

Figure 2 presents the static scheme and the diagrams of internal forces mobilized by the bending moment, $M$, acting on the cross section. The action of the bending moment makes the resultant forces appear in the compressed concrete region, $R_c$, and in the tensioned reinforcement region, $R_s$. The first one, is positioned at the centroid of the concrete strain-stress diagram, and the second one, at the geometric center of the reinforcement. The distance between the most compressed fiber of the section to the geometric center of the reinforcement is defined by the effective height, $d$. Usually, this distance is assumed to be $d = 0.9h$, with $h$ being the section height. The flat section hypothesis is admitted for this loading condition, even though the section is formed by two materials, as indicated in Figure 2. This hypothesis states that a section that was considered originally flat remains flat after deformation, including that of creep. It is important to note that, due to creep, all parameters related to concrete become implicit functions of time, as established in equations (8) e (17).

The resultant force of compression, $R_c$, is obtained by:

$$R_c = A_d b_w \tag{20}$$

where $A_d$ is the area of the stress-strain diagram and $b_w$ is the width of the beam. The resultant force on the reinforcement is given by:

$$R_s = f_{sd} A_s \tag{21}$$

where $f_{sd}$ is the design steel yield strength and $A_s$ is the total reinforcement area to be calculated. In the horizontal static balance, the resultants of concrete, $R_c$, and steel, $R_s$, are equal, because there is no movement of the section in that direction. Thus, it can be written that:

$$R_c = R_s \tag{22}$$

Therefore, from the equality derived from Eq. (22), the reinforcement steel area can be defined by Eq. (23):

$$A_s = \frac{A_d b_w}{f_{sd}} \tag{23}$$

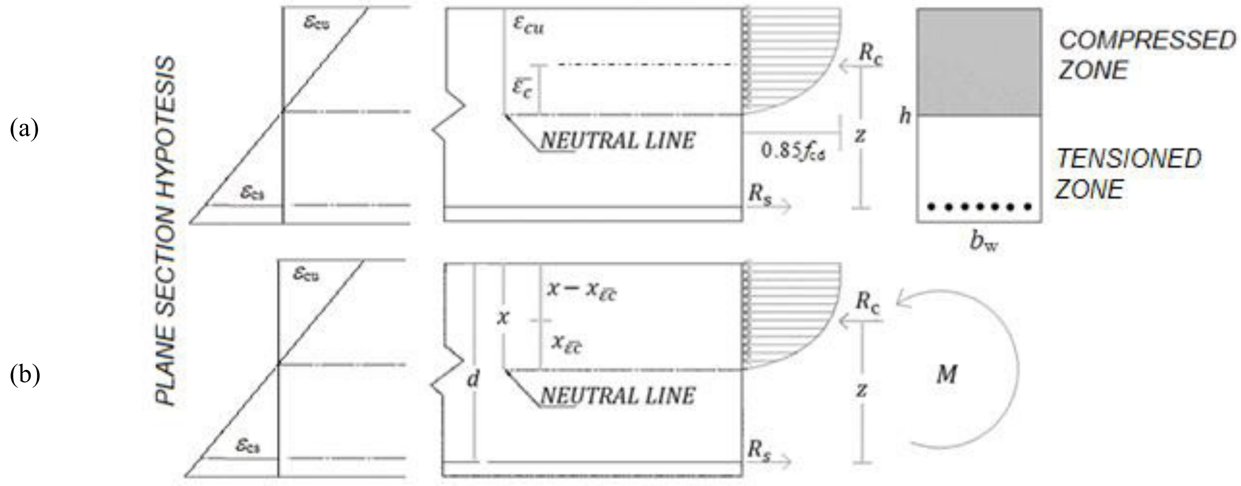


Figure 2. Rectangular beam sizing.

For the complete balance of the section to be established, the internal forces of concrete and reinforcement need to be equivalent, coplanar, but not collinear. This condition ensures the balance regarding both translational and rotational movements. The necessary condition for the equilibrium in rotation is that:

$$M_d = R_c z = R_s z \tag{24}$$

where $z$ represents the orthogonal distance, or lever arm, between the resultant forces of concrete and reinforcement, as indicated in Figure 2. With this, it can be written that:

$$M_d = A_d b_w z \tag{25}$$

Observing Figure 3, obtained from Figure 2, it is possible to establish geometrical relationships between heights and strains, in the section, which are:

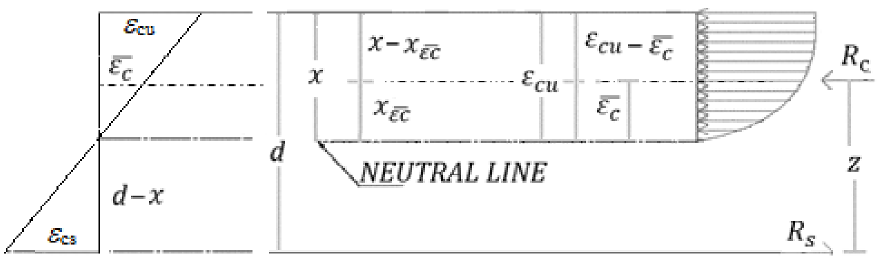


Figure 3. Rectangular beam sizing.

$$\frac{x}{\varepsilon_{cu}} = \frac{x - x_{\overline{\varepsilon_c}}}{\varepsilon_{cu} - \overline{\varepsilon_c}} \rightarrow (x - x_{\overline{\varepsilon_c}}) = x\frac{\varepsilon_{cu} - \overline{\varepsilon_c}}{\varepsilon_{cu}} \therefore (x - x_{\overline{\varepsilon_c}}) = x(1 - \frac{\overline{\varepsilon_c}}{\varepsilon_{cu}}) \tag{26}$$

where $x_{\bar{\varepsilon_c}}$ represents the distance related to strain $\bar{\varepsilon_c}$, $x$ is the distance from the neutral line to the most compressed fiber of the concrete, corresponding to strain $\varepsilon_{cu}$, and $x_{\overline{\varepsilon c}}$ is the centroid position, taken with reference to the neutral line. The area of the strain-stress diagram is obtained by replacing the strains in Eq. (6) by the respective distances in Eq. (26). With this, Eq. (27) is obtained:

$$A_d = 0.85 f_{cd} x \{1 + \frac{\varepsilon_{c2}[\left(1 - \frac{1}{n+1}\right) - 1]}{\varepsilon_{cu}}\} \tag{27}$$

The orthogonal distance between the line of action of the resultant force of concrete and that of steel is given by:

$$z = d - (x - x_{\overline{\varepsilon c}}) \tag{28}$$

Then, from Eq. (26), it can be done that:

$$z = d - x(1 - \frac{\bar{\varepsilon_c}}{\varepsilon_{cu}}) \tag{29}$$

With the previous expressions, Eq. (25) can be represented by a quadratic equation in the form of Eq. (30):

$$Ix^2 + Jx - M_d = 0, \qquad (0 < x \leq 0.5h) \tag{30}$$

where:

$$I = 0.85 f_{cd} b_w [1 + \frac{\frac{-\varepsilon_{c2}}{n+1}}{\varepsilon_{cu}}](\frac{\bar{\varepsilon_c}}{\varepsilon_{cu}} - 1) \tag{31}$$

and

$$J = 0.85 f_{cd} b_w d [1 + \frac{\frac{-\varepsilon_{c2}}{n+1}}{\varepsilon_{cu}}] \tag{32}$$

ABNT NBR 6118 establishes that the distance from the neutral line to the most compressed fiber, generally, cannot be greater than 50% of the cross-section height, in order to ensure the ductility of the structure. Therefore, the only admissible root of Eq. (30) is that between the null value and $0.5h$. Eqs. (31) and (32) represent the dependent $I$ and $J$ coefficients of the quadratic equation.

With the distance from the neutral line defined according to Eq. (30), it is necessary to return to Eq. (24) to obtain the expression for calculating the reinforcement steel area, $A_s$, in order to include the action of the bending moment. Thus:

$$M_d = f_{sd} A_s [d - x_{\varepsilon cu}(1 - \frac{\bar{\varepsilon_c}}{\varepsilon_{cu}})] \tag{33}$$

Therefore, the reinforcement steel area can be obtained from the expression in Eq. (34):

$$A_s = \frac{M_d}{f_{sd}[d - x(1 - \frac{\bar{\varepsilon_c}}{\varepsilon_{cu}})]} \tag{34}$$

which is a function of the bending moment on the section and the concrete strain-strain diagram parameters. The reinforcement area established by Eq. (34) is obtained without considering creep. To include it, Eq. (34) must express time dependence because concrete strains are, as in Eq. (17). Thus, the neutral line position also becomes a time-dependent one. Therefore, Eq. (34) must be written in the form of the Eq. (35):

$$A_s(t) = \frac{M_d}{f_{sd}[d - x(t)(1 - \frac{\bar{\varepsilon_c}(t)}{\varepsilon_{cu}(t)})]} \tag{35}$$

## 4. NUMERICAL SIMULATION

Taking into account the considerations described in the previous items and the need to include creep in the design of reinforced concrete structures in order to establish a reinforcement steel area compatible with the modified concrete diagram, a programming routine in Python language was used to implement the formulations described above. The parameters adopted in the simulation are shown in Table 1.

With the parameters indicated in Table 1, and assuming standard conditions for the concrete production, it was possible to generate the graphs in Figure 4, (a) stress-strain and (b) strain-strain, both considering the creep of the material. The results of the reinforcement area for different time instants, defined, in the present simulation, by mere convenience, can be seen in Table 2.

Table 1. Input parameters.

| **Parameter** | **Value** |
|---|---|
| Concrete characteristic strength C30 ($f_{ck}$) | 30 MPa |
| Steel grade CA50 ($f_{sk}$) | 500 MPa |
| Unfactored bending moment ($M$) | 250 kNm |
| Cross section width ($b_w$) | 30 cm |
| Cross section height ($h$) | 65 cm |
| Relative humidity of air ($H$) | 70 % |

Table 2. Stress-strain diagram parameters and reinforcement steel area.

| **Output parameter** | | ***t* (day)** | | | | | | |
|---|---|---|---|---|---|---|---|---|
| | | 0 | 28 | 100 | 500 | 1000 | 4000 | 20000 |
| $\boldsymbol{\sigma_c}$ (MPa) | $0.5f_{cd}$ | 10.71 | 10.71 | 10.71 | 10.71 | 10.71 | 10.71 | 10.71 |
| | $0.85f_{cd}$ | 18.21 | 18.21 | 18.21 | 18.21 | 18.21 | 18.21 | 18.21 |
| $\boldsymbol{\varepsilon_c}$ (x $10^{-3}$) | $\varepsilon_{c1}$ | 0.72 | 0.72 | 1.10 | 1.23 | 1.26 | 1.28 | 1.29 |
| | $\varepsilon_{c2}$ | 2.00 | 2.00 | 3.07 | 3.44 | 3.51 | 3.57 | 3.60 |
| | $\varepsilon_{cu}$ | 3.50 | 3.50 | 5.38 | 6.03 | 6.14 | 6.25 | 6.29 |
| $\boldsymbol{\bar{\varepsilon}_c}$ (x $10^{-3}$) | | 2.04 | 2.04 | 3,14 | 3.52 | 3.58 | 3.65 | 3.67 |
| $\boldsymbol{A_d}$ (MPa) | | 51.61 | 51.61 | 79.31 | 88.85 | 90.49 | 92.08 | 92.76 |
| $\boldsymbol{A_s}$ (cm$^2$) | | 15.42 | 15.42 | 23.70 | 26.55 | 27.04 | 27.52 | 27.72 |

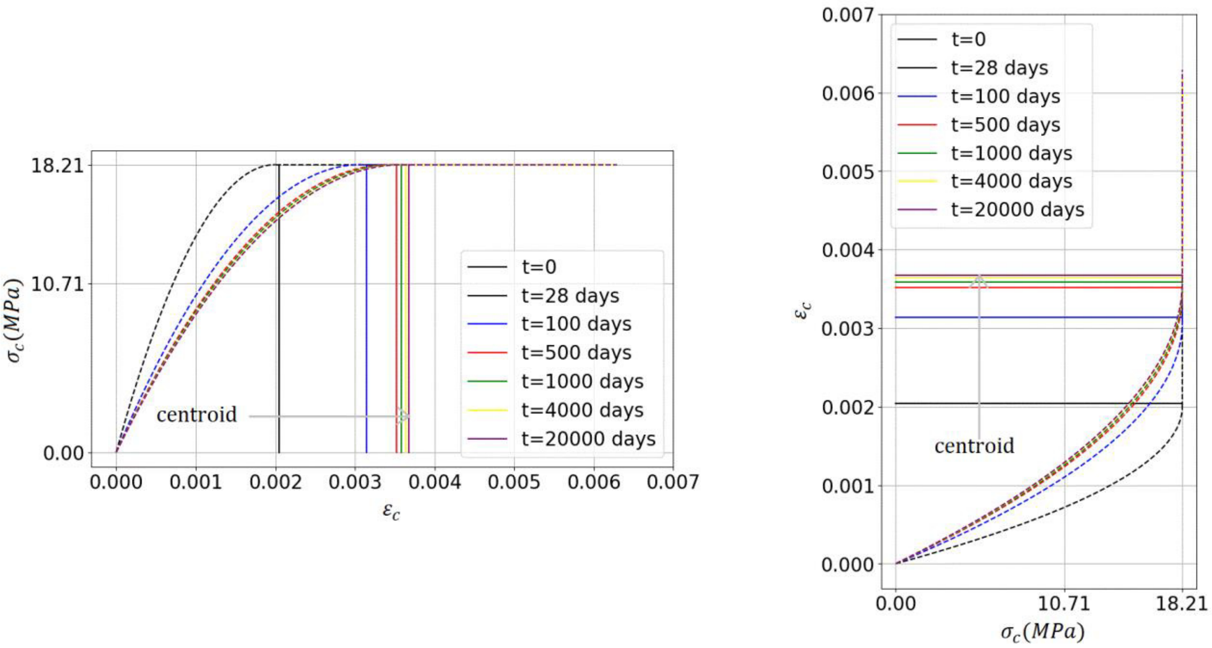


(a) (b)

Figure 4. Stress-strain (a) and strain-stress (b) diagrams of concrete considering creep.

Figure 5 describes the evolution of the steel reinforcement area calculation over time. For this simulation, the loading used refers to percentages ranging from 25% to 100% of the bending moment value defined in Table 1.

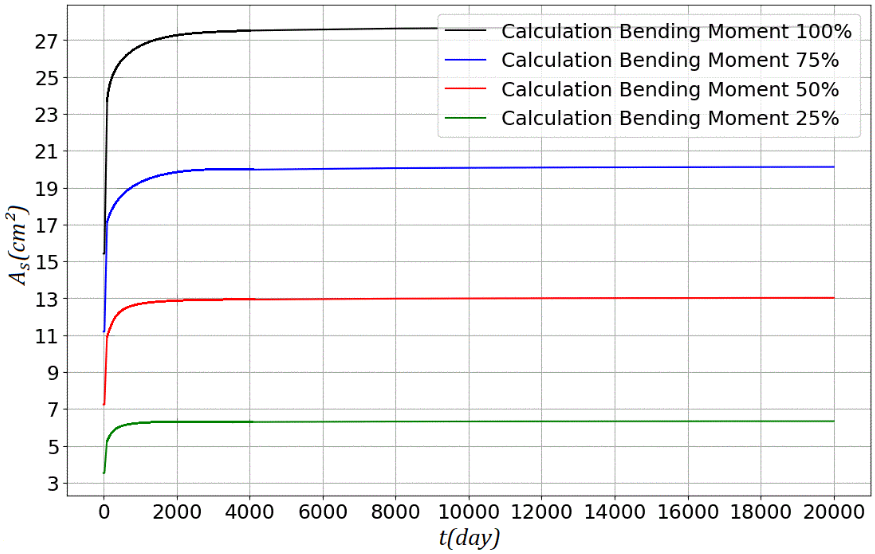


Figure 5. Steel area graph varying according to bending moment and time.

Table 3 details the results presented in the graph of Figure 5. It is possible to verify that, with the variation of time, the area of the stress-strain diagram increases and, consequently, the reinforcement steel area. As the structure ages, there is a need for a larger reinforcement area due to the transfer of stresses from concrete to reinforcement due to the material creep (Wahrhaftig, 2020; Wahrhaftig et al. 2023). Furthermore, there is a trend towards convergence of the calculated value of the reinforcement area around 4000 days after the structure is loaded.

Table 3. Reinforcement area according to the bending moment and time ($cm^2$).

| $M_d$ (kNm) | *t* (day) | | | | | | |
|---|---|---|---|---|---|---|---|
| | 0 | 28 | 100 | 500 | 1000 | 4000 | 20000 |
| 87.5 | 3.53 | 3.53 | 5.42 | 6.07 | 6.18 | 6.29 | 6.34 |
| 175.0 | 7.25 | 7.25 | 11.14 | 12.48 | 12.71 | 12.93 | 13.03 |
| 262.5 | 11.20 | 11.20 | 17.21 | 19.28 | 19.63 | 19.98 | 20.13 |
| 350.0 | 15.42 | 15.42 | 23.70 | 26.55 | 27.04 | 27.52 | 27.72 |

## 5. CONCLUSIONS

In this paper has been evaluated the change in the reinforcement steel area required for the balance of a reinforced concrete cross-section over time. The temporal analysis of the reinforcement area was necessary due to the inclusion of concrete creep in calculation. In the studied case, it was verified that there were variations in the reinforcement area throughout the analyzed period, reaching a maximum variation of 44% in relation to that calculated at the moment of loading. Another finding worth noting is the tendency for the steel reinforcement area to converge after 4000 days of the structure being put into service.

## 6. ACKNOWLEDGEMENTS

The authors would like to thank FAPESB, the Research Support Foundation of the State of Bahia; CNPq, the Brazilian National Council for Scientific and Technological Development; and CAPES, the Coordination of Superior Level Staff Improvement, for the research scholarships and support provided.

## 7. REFERENCES

ABNT, 2014, NBR 6118: Design of concrete structures – Procedure (in Portuguese), Associação Brasileira de Normas Técnicas ABNT, Rio de Janeiro.

ACI (American Concrete Institute), Prediction of creep, shrinkage, and temperature effects in concrete structures. ACI-209R-08, ACI Committee 209, Michigan, 2008.

Ali, S. A., and Forth, J. P., 2023. “Time-dependent behaviour of RC beams under eccentric combined loads as a unit of beam-column joint assemblies made from normal strength concrete without/with CFRP wraps”, *Engineering Structures*, Vol. 288, pp. 116221. DOI: 10.1016/j.engstruct.2023.116221.

Boumakis, I., Di Luzio, G., Marcon, M., Vorel, J. and Wan-Wendner, R., 2018. “Discrete element framework for modeling tertiary creep of concrete in tension and compression”, *Engineering Fracture Mechanics*, Vol. 200, pp. 263-282. DOI: 10.1016/j.engfracmech.2018.07.006.

Elaghoury, Z., and Bartlett, F. M., 2019. “Long-Term Deflections of Reinforced Concrete Beams”, *Proceedings of the CSCE Annual Conference*. Available in www.csce.ca/elf/apps/CONFERENCEVIEWER/conferences/2019/pdfs/PaperPDFversion_213_0425075250.pdf.

Giorla, A. B. and Dunant, C. F., 2018. “Microstructural effects in the simulation of creep of concrete”, *Cement and Concrete Research*, Vol. 105, pp. 44-53. DOI: 10.1016/j.cemconres.2017.12.001.

Magalhães, K. M. M., Brasil, R. M. L. R. F., Wahrhaftig, A. M., Siqueira, G. H., Bondarenko, I. and Neduzha, L. 2022. “Influence of Atmospheric Humidity on the Critical Buckling Load of Reinforced Concrete Columns”, *International Journal of Structural Stability and Dynamics*, Vol. 22, n. 1, p. 2250011. DOI. 10.1142/S0219455422500110.

Magalhães, K. M. M., Wahrhaftig, A. de M. and da Fonseca Brasil, R. M. L. R., 2023. “Strain regime induced by axial compression in slender reinforced concrete columns using different mathematical approaches”, *Structures*, Vol. 49, pp. 655-665. DOI: 10.1016/j.istruc.2023.01.148.

Nicoletti, V., Carbonari, S. and Gara, F., 2022. “Nomograms for the pre-dimensioning of RC beam-column joints according to Eurocode 8”, *Structures*, Vol. 39, pp. 958-973. DOI: 10.1016/j.istruc.2022.03.083.

Pena, P. V. C., dos Reis Ferreira, R. B., dos Santos, A. C., and de Oliveira, A. M., 2023. “Analysis of the compressive creep strain of the concretes with steel fibers: A holistic view in micro and macro scale”, *Journal of Building Engineering*, Vol. 71, pp. 106436. DOI: 10.1016/j.jobe.2023.106436.

Song, P.S. and Hwang, S., 2004. “Mechanical properties of high-strength steel fiber-reinforced concrete”, *Construction and Building Materials*, Vol. 18, n. 9, pp. 669-673. DOI: 10.1016/j.conbuildmat.2004.04.027.

Su, L., Wang, Y.-F., Mei, S.-q. and Li, P.-f., 2017. “Experimental investigation on the fundamental behavior of concrete creep”, *Construction and Building Materials*, Vol. 152, pp. 250-258. DOI: 10.1016/j.conbuildmat.2017.06.162.

Wahrhaftig, A. M., 2020. “Time-dependent analysis of slender, tapered reinforced concrete columns”, Steel and Composite Structures, Vol. 36, n. 2, pp 229-247. DOI: https://doi.org/10.12989/scs.2020.36.2.229.

Wahrhaftig, A. M., Magalhães, K. M. M., Brasil, R. M. L. R. F., 2023. Updating the bearing capacity, stresses, and strain for retrofitting reinforced concrete towers of the cellular and internet system, *Mechanics Based Design of Structures and Machines*, Vol. 51, n.1, pp 464-480. DOI: 10.1080/15397734.2020.1846559

Wei, Y., Wu, Z., Huang, J., and, Liang, S., 2018. “Comparison of Compressive, Tensile, and Flexural Creep of Early-Age Concretes under Sealed and Drying Conditions”, *Journal of Materials in Civil Engineering*, Vol. 30, n. 11, pp. 04018289. DOI: 10.1061/(ASCE)MT.1943-5533.0002495.

Yu, P., Duan, Y.H., Fan, Q.X. and Tang, S.W., 2020. “Improved MPS model for concrete creep under variable humidity and temperature”, *Construction and Building Materials*, Vol. 243, pp. 118183. DOI: 10.1016/j.conbuildmat.2020.118183.

Zamaliev, F.S. and Zakirov, M.A., 2018. “Stress-strain state of a steel-reinforced concrete slab under long-term.” Magazine of Civil Engineering, Vol. 83, n. 7, pp. 12–23. DOI: 10.18720/MCE.83.2.

Zhou, Y., Chen, W. and Yan, P., 2022. “Measurement and modeling of creep property of high-strength concrete considering stress relaxation effect”, *Journal of Building Engineering*, Vol. 56, pp. 104726. DOI: 10.1016/j.jobe.2022.104726.

## 8. RESPONSIBILITY NOTICE

The authors are solely responsible for the printed material included in this paper.